British Journal of Pharmacology (2008) 154, 890–900

0007–1188/08 $30.00
www.brjpharmacol.org

RESEARCH PAPER

Examination of signalling pathways involved in muscarinic responses in bovine ciliary muscle using YM-254890, an inhibitor of the $G_{q/11}$ protein

F Yasui[1,4], M Miyazu[2,4], A Yoshida[1], K Naruse[3] and A Takai[2]

[1]*Department of Ophthalmology, Asahikawa Medical College, Hokkaido, Japan;* [2]*Department of Physiology, Asahikawa Medical College, Hokkaido, Japan and* [3]*Department of Cardiovascular Physiology, Okayama University Graduate School of Medicine, Dentistry and Pharmaceutical Sciences, Okayama, Japan*

Background and purpose: In the ciliary muscle, the tonic component of the contraction produced by cholinergic agonists is highly dependent on Ca^{2+} provided by influx through non-selective cation channels (NSCCs) opened by stimulation of M_3 muscarinic receptors. We examined effects of YM-254890 (YM), a $G_{q/11}$-specific inhibitor, on contraction, NSCC currents and $[Ca^{2+}]_i$ elevation induced by carbachol (CCh).
Experimental approach: Isometric tension was recorded from ciliary muscle bundles excised from bovine eyes. In ciliary myocytes dispersed with collagenase and cultured for 1–5 days, whole-cell currents were recorded by voltage clamp and the intracellular free Ca^{2+} concentration $[Ca^{2+}]_i$ was monitored using the Fluo-4 fluorophore. Existence and localization of M_3 receptors and the α subunit of $G_{q/11}$ ($G\alpha_{q/11}$) were examined by immunofluorescence microscopy using AlexaFluor-conjugated antibodies.
Key results: Both phasic and tonic components of contractions evoked by 2 μM CCh were inhibited by YM (3–10 μM) in a dose-dependent manner. In the cultured cells, CCh (0.05–10 μM) evoked an NSCC current as well as an elevation of the $[Ca^{2+}]_i$. Both initial and sustained phases of these CCh-evoked responses were abolished by YM (3–10 μM). Immunostaining of the cytoplasmic side of the plasma membrane of ciliary myocytes revealed a dense distribution of M_3 receptors and $G\alpha_{q/11}$.
Conclusions and implications: The tonic as well as phasic component of the ciliary muscle contraction appears to be under control of signals conveyed by a $G_{q/11}$-coupled pathway. YM is a useful tool to assess whether $G_{q/11}$ is involved in a signal transduction system.
British Journal of Pharmacology (2008) **154**, 890–900; doi:10.1038/bjp.2008.140; published online 21 April 2008

Keywords: ciliary muscle; muscarinic agents; GTP-binding proteins; $G_{q/11}$ inhibitor; visual accommodation

Abbreviations: $[Ca^{2+}]_i$, intracellular Ca^{2+} concentration; CCh, carbachol; DAG, diacylglycerol; NSCC, non-selective cation channel; OAG, 1-oleyl-2-acetyl-*sn*-glycerol; PIPES, 1,4-piperazinediethanesulphonic acid; PSS, physiological saline solution; TRPC, canonical transient receptor potential; YM, YM-254890

Introduction

In the eye of mammalian species, the force required for the fine and stable adjustment of the focus of the lens is provided by contraction of a specialized smooth muscle called the ciliary muscle. The innervation of this muscle is almost exclusively parasympathetic, and its contraction is initiated and sustained by stimulation of muscarinic receptors mainly of the M_3 subtype (Alexander *et al.*, 2007) on the surface of the muscle cell membrane by the neurotransmitter ACh (Glasser and Kaufman, 2003). It is generally thought that the initial phasic component of the contraction is triggered by intracellular Ca^{2+} release mediated by a $G_{q/11}$-linked signalling pathway (see Masuda *et al.*, 1998). The ensuing tonic phase of the contraction requires continuous replenishment of internal Ca^{2+} by influx from the extracellular space. However, as demonstrated in the bovine and human (Suzuki, 1983) and in the canine species (Ito and Yoshitomi, 1986), the ciliary muscle lacks, or is deficient in, voltage-gated Ca^{2+} entry pathways. In previous experiments on the bovine ciliary muscle, we have identified two non-selective cation channels (NSCCs) with different unitary conductances (35 pS and 100 fS), which are opened upon stimulation of M_3 receptors, and have shown that the Ca^{2+} influx through either or both of these NSCCs is responsible

Correspondence: Professor A Takai, Department of Physiology, Asahikawa Medical College, Midorigaoka-Higashi 2-1-1-1, Asahikawa 078-8510, Hokkaido, Japan.
E-mail: takai@asahikawa-med.ac.jp
[4]These authors contributed equally to this work.
Received 4 December 2007; revised 18 February 2008; accepted 4 March 2008; published online 21 April 2008

for the tonic phase of contraction produced by muscarinic stimulation (Takai *et al*., 2004; Sugawara *et al*., 2006). However, little is known about how signals are transmitted from the receptor to the NSCCs to induce the Ca^{2+} influx.

Recently, it has been reported that YM-254890 (YM), a cyclic depsipeptide of 960.08 Da (molecular formula, $C_{46}H_{69}N_7O_{15}$) produced by a *Chromobacterium* species, specifically binds to the α-subunit of $G_{q/11}$ protein ($G\alpha_{q/11}$) and inhibits its signalling activity (Takasaki *et al*., 2004; Uemura *et al*., 2006). In the present experiments, we examined effects of this $G_{q/11}$ inhibitor on tension development, intracellular Ca^{2+} concentration ($[Ca^{2+}]_i$) elevation and NSCC currents evoked by a muscarinic agent, carbachol (CCh). To examine the existence and localization of M_3 receptors and $G\alpha_{q/11}$ in ciliary muscle cells, we conducted immunofluorescence microscopy using antibodies specific to these proteins. We show here that YM (0.01–10 μM) inhibits both the initial peak and the tonic plateau of the CCh-evoked responses, in a dose-, time- and temperature-dependent manner. We also show results which suggest that signals transmitted by the M_3 receptor-$G_{q/11}$ pathway induce enhancement of the contractility at a given level of $[Ca^{2+}]_i$ (that is, Ca^{2+} sensitization) in bovine ciliary muscle. Our microscopic study confirms the abundant distribution of M_3 receptor and $G\alpha_{q/11}$ in the plasma membrane of ciliary myocytes or on its cytoplasmic surface. In summary, we propose that the tonic as well as the phasic component of the ciliary muscle contraction is under control of signals conveyed by a $G_{q/11}$-coupled pathway.

Methods

Tissue preparation and cell culture

Bovine eyes were enucleated soon after the animals were killed in a local slaughterhouse and transported to our laboratory in ice-cold physiological saline solution (PSS). The eyes were incised circumferentially about 5 mm posterior to the limbus, and after the vitreous humour and lens were removed, the ciliary muscle was carefully dissected out from the scleral spur.

Single muscle cells were obtained by the method previously described (Takai *et al*., 1997). Briefly, the excised muscle was equilibrated in nominally Ca^{2+}-free PSS containing 100 mM K^+ at 35 °C for 30 min and transferred to a solution of the same composition supplemented with 0.4% (w/v) collagenase (Wako Junyaku Co., Tokyo, Japan) and 0.02% (w/v) papain (Sigma Chemical Co., St Louis, MO, USA). After incubation for 20–25 min, the cell suspension was filtered through a fine nylon mesh. The dispersed cells were collected by centrifuging at 200 *g* for 2 min and then resuspended in nominally Ca^{2+}-free, high K^+ (100 mM) PSS. The isolated cells were cultured on a glass surface in a serum-free HAM F12 media (Sigma) for 1–5 days before use for experiments. Glass-bottomed dishes (35 mm in diameter; for calcium measurements) and small glass plates (5 mm × 5 mm in size and 0.2 mm in thickness; for electrophysiological experiments) used in this culturing procedure were coated with fibronectin (Sigma; cat code, F2006).

Mechanical recordings

The methods of tension recording and of superfusion were essentially the same as previously described (Takai *et al*., 2004). Briefly, a small piece (about 1 mm wide and 5 mm long) of smooth muscle was carefully dissected from an excised ciliary muscle bundle under a binocular microscope. The preparation was vertically mounted in a small organ bath (0.5 mL in volume) through which solution flowed at a constant rate of 2 mL min^{-1}. The tension was isometrically recorded using a U-gauge transducer (type UL-2GR; Minebea Co., Tokyo, Japan) and an LC240 load-cell converter (Unipulse Co., Tokyo, Japan) connected to a potentiometric pen recorder. For graphing and analysis purposes, the pen-recorder traces were digitized using an image scanner and the DigiMatic software (FEB Software, Chesterfield, VA, USA).

Recordings of intracellular calcium concentration

A digital CCD Fluorescence Microimaging System (Olympus Co., Tokyo, Japan) was used for recordings of intracellular calcium concentration ($[Ca^{2+}]_i$) as well as for immunofluorescence microscopy (see below). To monitor the changes of the $[Ca^{2+}]_i$, cultured ciliary myocytes were loaded with Fluo-4/AM (MDS Sciex Co., Concord, ON, Canada). Excitation was achieved using a 100 W Hg lamp with a 460–495 nm band-pass filter and the fluorescence emitted thereby was recorded from macroscopic single-cell image regions after 510–550 nm band-pass filtering. Experiments were carried out at room temperature (25 ± 1 °C).

The $[Ca^{2+}]_i$ was calculated from the fluorescence intensity, *F*, using the conversion equation (Takahashi *et al*., 1999)

$$[Ca^{2+}]_i = K_D \cdot \frac{F - F_{min}}{F_{max} - F} \quad (1)$$

where K_D (= 345 nM) is the dissociation constant for the interaction of Fluo-4 with Ca^{2+}, and F_{max} and F_{min} are the maximal and minimal values of the fluorescence intensity, respectively (see Figure 5).

Electrical recordings

An Axopatch 200B amplifier (Axon Instruments, Foster City, CA, USA) was used for whole-cell voltage clamp experiments. The borosilicate glass pipettes used were made by a PC-10 puller (Narishige Co., Tokyo, Japan). The pulling condition was routinely set so that the pipettes had a tip resistance of 12–15 MΩ when filled with the pipette solution. For intracellular application of GTPγS, the tip resistance setting was lowered to 5–8 MΩ to make diffusional movement of the substance into the cell faster and more effective (see Figure 7). For command pulse generation and digital data acquisition, we used a Digidata 1200B interface controlled by the pClamp software (version 9.2; Axon Instruments) running on a Windows-based computer. Relatively short sections of data were recorded on a magnetopic disk after online digitization. Long sections of data were recorded on a video cassette using a VR-10B PCM converting system (Instrutech Co., Long Island, NY, USA). Mathematical processing and analysis of data were carried out using the ClampFit software (version

9.2; Axon Instruments) and the Origin software (version 7.5; OriginLab, Northampton, MA, USA).

For non-stationary variance analysis, the whole-cell current signal was filtered by an analogue four-pole Bessel filter at 1 kHz (−3 dB) and digitized at 2 kHz, before the mean μ and the variance σ^2 around the mean were calculated for every 1000 sample points. If the open-state probability of the channel whose openings give rise to the current is sufficiently small, then:

$$\sigma^2 = \zeta\mu + \sigma_0^2 \quad (2)$$

where ζ denotes the unitary current amplitude and σ_0^2 represents the contributions from undesired fluctuations such as thermal noise of the voltage clamp (see for example, Sigworth, 1980). For NSCCs in which the polarity of the current is reversed at a near-zero voltage, one can reasonably assume that $\zeta = E_h\gamma$, where E_h is the holding potential and γ is the unitary conductance.

Immunofluorescence microscopy

After 4- to 5-days culture of bovine ciliary muscle cells on the surface of fibronectin-coated glass plates, the body of the cells was removed by gentle pulse sonication using a VP-5S Microsonicator (Taitec Co., Koshigaya, Saitama, Japan) in a hypotonic solution containing 10 mM 1,4-piperazinediethanesulphonic acid (PIPES), 10 mM $MgCl_2$ and 0.5 mM EGTA (pH 7.2, adjusted with NaOH). Unless otherwise mentioned, the cytoplasmic side of the plasma membrane remaining attached on the glass surface after this procedure was fixed by exposing to phosphate-buffered saline supplemented with 4% paraformaldehyde for 5 min and then well rinsed with phosphate-buffered saline containing no paraformaldehyde, before they were treated with primary antibodies (final concentration, 2.5–5 $\mu g\,mL^{-1}$). Of the primary antibodies used in the present experiments, the polyclonal anti-$G\alpha_{q/11}$-rabbit IgG and the polyclonal anti-M_3R goat IgG were purchased from Santa Cruz Biotechnology Inc., Santa Cruz, CA, USA (catalogue code, sc-392 and sc-7474). The monoclonal anti-α-actin mouse IgG were a product of Progen Biotechnik GmbH, Heidelberg, Germany (catalogue code, 65001). To visualize the primary antibody for $G\alpha_{q/11}$, we used as the secondary antibody an anti-rabbit-IgG donkey IgG conjugated with AlexaFluor 546 (Invitrogen, Carlsbad, CA, USA; peak absorption and emission at 556 and 573 nm, respectively). The primary antibodies for M_3 receptor and α-actin were visualized using an anti-goat-IgG donkey IgG and an anti-mouse-IgG goat IgG, respectively, both of which were conjugated with AlexaFluor 488 (Invitrogen; peak absorption and emission at 496 and 524 nm, respectively).

Analysis of concentration–inhibition relationships

To describe a concentration–inhibition relationship, we routinely use the Hill function

$$\phi(x) = \frac{K^h}{K^h + x^h}\,\phi(0) \quad (3)$$

where $\phi(x)$ is the intensity of response in the presence of the inhibitor whose concentration is x (which may be zero), K denotes the apparent dissociation constant and h (>0) stands for the Hill coefficient. To estimate the values of K and h with standard errors, we fit Equation (3) to the data by nonlinear least-squares regression, using as weight the reciprocal of the square of the standard error at each value of x.

Statistics

Comparison of two numerical data sets was performed by a generalized Student's *t*-test in either paired or unpaired manner depending on the cases (Snedecor and Cochran, 1980; Carroll and Ruppert, 1988). Two-way ANOVA was carried out to compare time-course data (Snedecor and Cochran, 1980). Differences were taken as statistically significant when two-tailed probabilities less than 0.05 were obtained.

Solutions and chemicals

The normal PSS used was of the following composition (mM): NaCl, 127; KCl, 5.9; $CaCl_2$, 2.4; $MgCl_2$, 1.2; glucose, 11.8; HEPES, 10. The pH was adjusted to 7.4 by titration with 1 N NaOH at temperatures at which experiments were carried out. High K^+ (100 mM) PSS was prepared by replacing NaCl with equimolar KCl.

Unless otherwise mentioned, pipettes for whole-cell voltage-clamp experiments (see below) were filled with a solution containing (mM): NaCl, 5; Cs aspartate, 100; $MgCl_2$, 5; ATP (disodium salt), 5; HEPES, 20; 1,2-bis(2-aminophenoxy)ethane-*N*,*N*,*N*′,*N*′-tetraacetic acid (BAPTA), 5 and GTP, 0.18. The pH was adjusted to 7.4 with NaOH.

Phosphate-buffered saline (pH 7.4) used for preparation of the membrane samples for immunofluorescence microscopy contained (mM): NaCl, 137; Na_2HPO_4, 8.10; KH_2PO_4, 1.47 and KCl, 2.68.

Carbamylcholine chloride (CCh), atropine sulphate, pirenzepine dichloride, GTP, PIPES, EGTA and 1-oleyl-2-acetyl-*sn*-glycerol (OAG) were purchased from Sigma Chemical Co. BAPTA was a product of Dojindo Co. (Tabaru, Kumamoto, Japan). YM was a gift from Astellas Pharmaceutical Co. (Tokyo, Japan). All other chemicals used were of analytical grade.

Results

Effects of YM on CCh-induced contraction

Figure 1a shows a typical pattern of isometric contraction of a bovine ciliary muscle bundle produced by prolonged application of CCh (2 μM) in normal PSS at 37 °C. The CCh-induced contraction showed an initial phasic component followed by a tonic component, which was maintained for longer than 3 h with only a slight decline (Figure 1a; see also ○ of Figure 3a). Application of 30 nM to 1 μM of YM during the tonic phase of the CCh-induced contraction caused a reduction of the tension in a dose-dependent manner (Figures 1b–d). Development of this inhibitory effect of YM followed a relatively slow time course, which cannot be fitted with a simple exponential function. At 100 nM YM (Figure 1c), for example, there was a time lag of 10–15 min

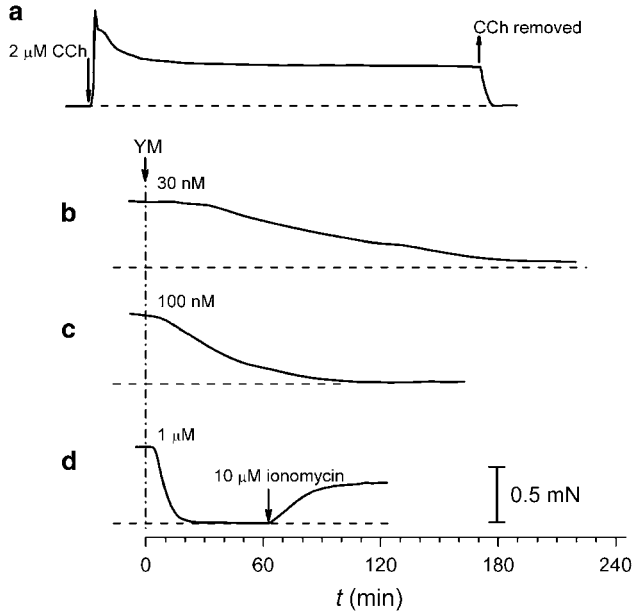

Figure 1 Carbachol (CCh)-induced contraction of the bovine ciliary muscle and its inhibition by YM-254890 (YM). Contraction induced by superfusion of 2 μM CCh at 37 °C was isometrically recorded in bovine ciliary muscle bundles. In the absence of the inhibitor (**a**), the CCh-induced contraction showed an initial phasic component followed by a tonic component that was maintained for longer than 3 h with only a slight decline. Superfusion of 30 nM (**b**), 100 nM (**c**) and 1 μM (**d**) of YM (at time, $t = 0$ min) during the tonic phase of the contraction caused a reduction of the tension in a dose-dependent manner. Development of this inhibitory effect of YM was slow particularly at lower inhibitor concentrations. In (**d**), note the tension development produced by addition of 10 μM ionomycin after complete inhibition of CCh-induced contraction by the treatment with 1 μM YM. Recordings (**a**–**d**) are from different ciliary muscle bundles.

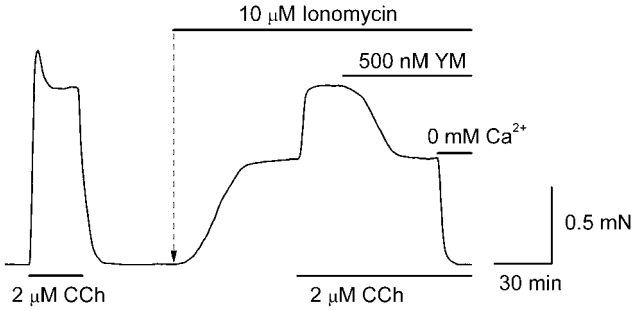

Figure 2 Additive effect of carbachol (CCh) on ionomycin-induced contraction and its inhibition by YM-254890 (YM). The effect of adding CCh (2 μM) during contraction induced by ionomycin (10 μM). In a preparation which gave a typical contractile response to CCh (the reference response), superfusion of ionomycin in the absence of CCh caused a slow tension development whose plateau level was only about 50% of the tonic level of the reference response (cf. Figure 1d). Addition of 2 μM CCh during the plateau of the ionomycin-induced contraction caused an increase in the tension, which approached the tonic level of the reference response. YM (500 nM) brought the tension augmented by adding CCh down to, but not below, the level before the addition of CCh. Removal of Ca^{2+} (+2 mM EGTA) in the presence of 10 μM ionomycin, 2 μM CCh and 500 nM YM caused a rapid and complete relaxation.

before the decline of the tension started to follow a single exponential time course with a time constant of 30 ± 3 min ($n = 5$; regression lines not shown). The tendency of time dependence was particularly marked at lower inhibitor concentrations (see also Figure 3 below). The meaning of the biphasic nature of the time course is not clear from the present experiments.

As shown in Figure 1d, superfusion of a Ca^{2+} ionophore, ionomycin (10 μM) (Williams *et al.*, 1985), after complete inhibition of the CCh-induced contraction by 1 μM YM, produced a sustained contraction. The plateau level intensity of this contraction was 53 ± 6% of the level of the tonic component of the contraction induced by 2 μM CCh in the same muscle (total number of experiments, $n = 7$). As shown in Figure 2, ionomycin (10 μM) produced a similar contractile response when applied to intact muscle preparations in the absence of muscarinic stimulation. Here, the plateau level intensity was 55 ± 5% ($n = 10$) of the tonic level of the contraction induced by 2 μM CCh alone. This percentage is comparable with, but not significantly larger than, the value given above for the contraction induced by the same concentration of ionomycin after the treatment with YM (see Figure 1d). These observations support the notion that YM has little, if any, effect on the intracellular contractile machinery.

Figure 2 also shows an additive effect of CCh on the contraction induced by ionomycin and its inhibition by YM. The slow tension development caused by 10 μM ionomycin required more than 30 min to reach a plateau (Figure 2; total number of experiments, $n = 10$). Addition of 2 μM CCh during this plateau phase caused an increase in the tension, which approached within 5 min the tonic level of the contraction produced by 2 μM CCh alone (Figure 2; $n = 5$). The ionomycin-induced contraction augmented by CCh was brought down to, but not below, the level before the addition of CCh, when 500 nM YM was added (Figure 2; $n = 5$). Removal of Ca^{2+} (2 mM EGTA) in the presence of 10 μM ionomycin, 2 μM CCh and 500 nM YM resulted in a fast and complete relaxation (Figure 2; $n = 5$). Essentially the same results were obtained when 20 μM ionomycin was used (examined in three preparations; data not shown). These observations may suggest the existence of Ca^{2+} sensitization mechanism(s) activated by the signals conveyed from M_3 receptors though $G_{q/11}$ in the bovine ciliary muscle (see Discussion).

As shown in Figure 3, the sensitivity of the CCh (2 μM)-induced contraction to YM decreased when the bath temperature was lowered. At 37 °C, a slight but significant inhibition ($P < 0.001$; two-way ANOVA) was observed at 10 nM YM, and a complete inhibition resulted within 90 min at 100 nM YM (Figure 3a). At 25 °C, however, 10 and 30 nM YM produced no significant effect, whereas 300 nM YM required 120 min to cause a complete inhibition (Figure 3b). The lower sensitivity of the ciliary muscle to YM at 25 °C compared with 37 °C may be due in part to a reduction of the membrane permeability to YM (see Discussion). The effects of changing the temperature on the inhibition of the CCh-induced contractions by YM have not been examined further.

In the experiments illustrated in Figure 4, sustained contraction produced by 2 μM CCh was completely suppressed by superfusion of 500 nM YM (at 37 °C). No contraction was evoked when CCh was re-applied in the

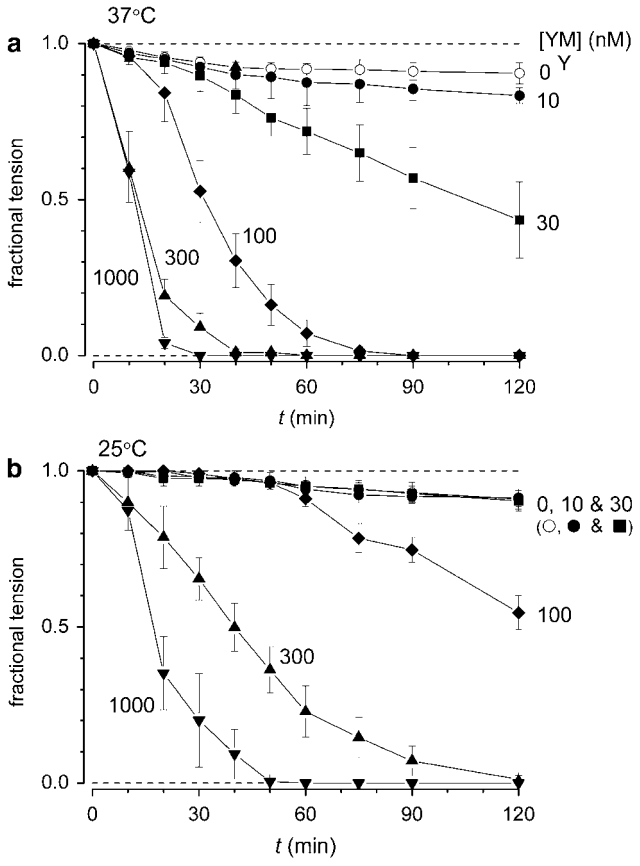

Figure 3 Temperature dependence of the inhibitory effect of YM-254890 (YM) on the carbachol (CCh)-induced contraction. In the same type of mechanical experiments as those shown in Figure 1, the inhibitory effect of different concentrations of YM on the tonic phase of contractions produced by 2 μM CCh was examined at 37 °C (**a**) and 25 °C (**b**). The tension level from the basal line was measured from pen-recorder traces at 10- to 60-min intervals. The values are normalized to the tension just before the application of YM ($t = 0$ min). The concentrations of YM applied were 0 nM (control), 10, 30, 100, 300 nM and 1 μM. Each symbol represents the mean of at least three values. Vertical bars indicating the s.e.mean are omitted if within symbols. The time course of the inhibition was markedly slower at 25 °C than at 37 °C, particularly at lower YM concentrations.

presence of YM (Figure 4). Thus, YM inhibited the phasic component as well as the tonic component of the CCh-induced contraction. The contractile responsiveness to CCh abolished by YM slowly recovered when the muscle was continuously washed with normal PSS (Figure 4). The recovery of the contractility after removal of YM, which was monitored by measuring the peak level of the contractions in response to repeated applications of CCh (2 μM) for 10 min at 50-min intervals, followed a single exponential time course (Figure 4, dashed curve; time constant, $\tau = 140 \pm 4$ min, $n = 6$). The tonic component also slowly recovered as evidenced by the final response produced by a prolonged (50 min) application of CCh (Figure 4).

Inhibitory effect of YM on the CCh-induced elevation of $[Ca^{2+}]_i$

As shown in Figure 5, YM also inhibited the tonic phase of CCh-induced elevations of $[Ca^{2+}]_i$ in cultured ciliary muscle

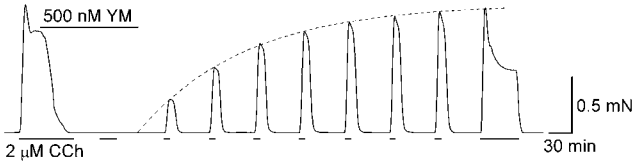

Figure 4 Recovery of the carbachol (CCh)-evoked contractility after wash-off of YM-254890 (YM). Sustained contraction was produced by stimulation with 2 μM CCh, and it was completely suppressed by superfusion of 500 nM YM. Readmission of CCh in the presence of YM caused no response. The abolished responsiveness to CCh was slowly recovered after YM was removed. The recovery, monitored by measuring the peak level of the contractions in response to CCh (2 μM) application for 10 min at 50-min intervals, followed a single exponential time course (dashed curve) with a time constant, $\tau = 140$ min. Note the recovery of the tonic component in the contraction produced by a prolonged (60 min) application of the same concentration of CCh at the end of the experiment.

cells. To monitor the $[Ca^{2+}]_i$, the intensity of fluorescence, *F*, of Fluo-4-loaded cells was recorded at 25 °C (Figure 5a). The $[Ca^{2+}]_i$ was calculated from the recorded values of *F*, using Equation (1) (Figure 5b). The maximal value of *F*, F_{max}, required for this calculation was determined as the level of *F* in the presence of 10 μM ionomycin (see Figure 5a). Superfusion of CCh (2 μM) evoked an elevation of $[Ca^{2+}]_i$, which showed an initial peak followed by a plateau (Figure 5b). On average, the plateau level of $[Ca^{2+}]_i$ was 263 ± 25 nM (number of cells examined, $n = 40$). The $[Ca^{2+}]_i$ was brought from this level down to but not below the level before the stimulation by CCh (dashed line) about 1 min after the start of superfusion of 5 μM YM. Relatively high concentrations (> 1 μM) of YM were required to produce a clear inhibition within 5 min. This is due presumably to the fact that these experiments were carried out at 25 °C and the considerable temperature dependence of the inhibitory effects of YM (see Figure 3).

YM also inhibited the phasic component of the CCh-induced $[Ca^{2+}]_i$ elevation, as shown in Figure 6. Relatively short (30 s) application of CCh (2 μM) produced a peaky rise of the $[Ca^{2+}]$, and this was abolished in the presence of 5 μM YM (observations in 13 cells).

In Figure 7, we examined the effects of removing Ca^{2+} from the superfusing solution (Figures 7a and b) and of adding atropine (Figure 7c), La^{3+} (Figure 7d) or nifedipine (Figure 7e) on the CCh-induced $[Ca^{2+}]_i$ elevation.

As shown in Figure 7a, removal of Ca^{2+} from the superfusing solution (2 mM EGTA) caused, in 12 of the 15 cells examined, a small transient elevation of $[Ca^{2+}]_i$, which was followed by a decrease to a basal level (dashed line) slightly lower than the level before the Ca^{2+} removal. Application of 2 μM CCh under this condition caused a clear phasic elevation of $[Ca^{2+}]_i$, but no tonic rise was observed until Ca^{2+} (2.4 mM) was readmitted in the presence of CCh (Figure 7a). Removal of Ca^{2+} was also very effective in abolishing the tonic phase of the CCh-induced $[Ca^{2+}]_i$ elevation (Figure 7b). These findings clearly indicate that the initial peak of the CCh-induced elevation of $[Ca^{2+}]_i$ in normal PSS is due to release from intracellular stores, whereas its plateau phase is produced by influx from the extracellular space through the cell membrane.

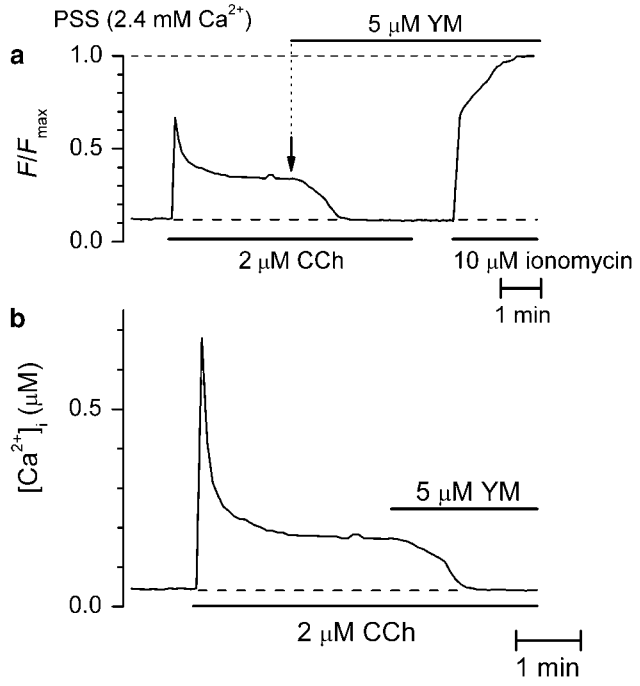

Figure 5 Carbachol (CCh)-induced elevation of $[Ca^{2+}]_i$ and inhibition of its tonic phase by YM-254890 (YM). Changes of $[Ca^{2+}]_i$ were monitored in cultured bovine ciliary muscle cells using Fluo-4 as the indicator at 25 °C. (**a**) The time course of the changes of fluorescence intensity, *F*, caused by superfusion of CCh (2 μM), YM (5 μM) and ionomycin (10 μM) and high Ca^{2+} (10 mM). (**b**) The changes of the $[Ca^{2+}]_i$ calculated from the data shown in (**a**), using equation (1). The maximal fluorescence intensity, F_{max}, was determined by the superfusion of 10 μM ionomycin in the presence of 10 mM Ca^{2+} (see **a**), and the minimal fluorescence intensity, F_{min}, was assumed to be 0.01 F_{max}. Superfusion of CCh (2 μM) evoked an elevation of $[Ca^{2+}]_i$, which showed an initial peak followed by a plateau. The $[Ca^{2+}]_i$ was brought down to, but not below, the level before the stimulation by CCh (see **b**, dashed line) in about 1 min after the start of superfusion of 5 μM YM.

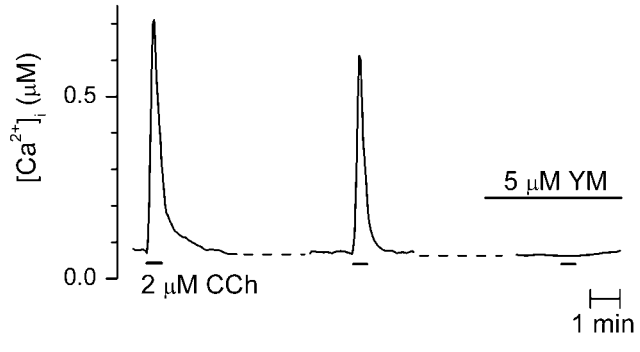

Figure 6 Inhibition of the carbachol (CCh)-induced phasic elevation of $[Ca^{2+}]_i$ by YM-254890 (YM). In the same type of experiment as described in Figure 5, the effect of YM was examined on the initial phase of CCh-induced rise of $[Ca^{2+}]_i$. CCh (2 μM) was applied to cultured myocytes three times for 30 s each at 7.5-min intervals. The first application of CCh evoked a sharp rise to a peak of $[Ca^{2+}]_i$. The second application produced a comparable, albeit slightly smaller, response. The third application, which was carried out 3 min after the start of superfusion of 5 μM YM, elicited no change in the $[Ca^{2+}]_i$. A set of recordings from a representative cell are shown.

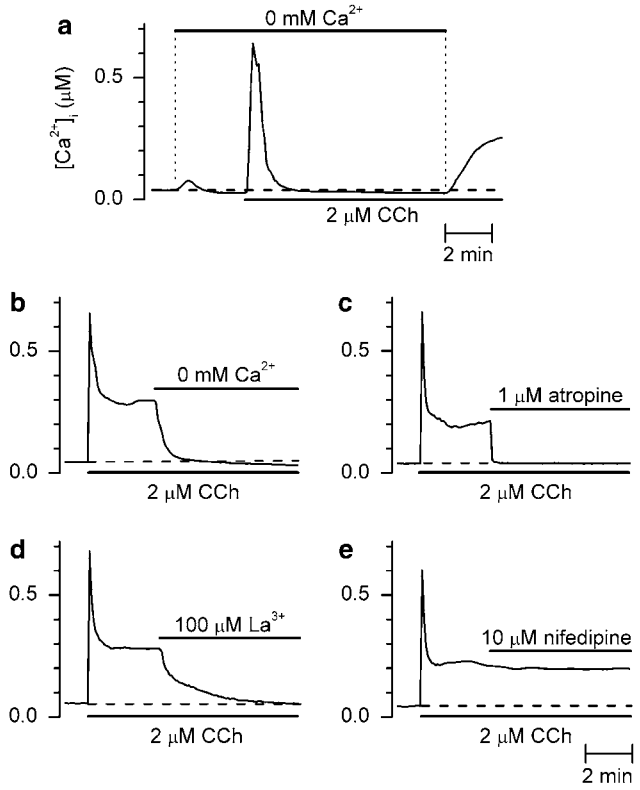

Figure 7 Effects of Ca^{2+} removal, and of adding atropine, La^{3+} and nifedipine on the CCh-induced $[Ca^{2+}]_i$ elevation. Changes of the $[Ca^{2+}]_i$ were recorded in cultured ciliary myocytes, as shown in Figure 5. (**a**) In the absence of Ca^{2+} (0.2 mM EGTA) in the extracellular space, superfusion of CCh (2 μM) caused only a transient increase in the $[Ca^{2+}]_i$. In normal physiological saline solution (PSS) (which contains 2.4 mM Ca^{2+}), the initial phasic increase in the $[Ca^{2+}]_i$ induced by CCh (2 μM) was followed by a plateau, as also seen in Figure 5b. Removal of Ca^{2+} (**b**) during the plateau phase caused a decrease of the $[Ca^{2+}]_i$ to a level below the level before the CCh application (dashed line). Superfusion of 1 μM atropine (**c**) or 100 μM La^{3+} (**d**) also suppressed the plateau of the CCh-induced response. The inhibitory effect of atropine was particularly quick. Nifedipine (10 μM, **e**) was without effect. Recordings (**a**–**e**) are from different cells at 25 °C, and each is representative of at least five independent experiments.

The plateau phase of the CCh-induced $[Ca^{2+}]_i$ elevation was quickly and completely suppressed by 1 μM atropine (observed in seven cells; Figure 7c shows a representative result). La^{3+} also inhibited the tonic phase, although a relatively high concentration (100 μM) was required for complete blockade (Figure 7d). As shown in Figure 8, the dose dependence of this inhibitory effect of La^{3+} was fitted by Equation (3) with $K = 7 \pm 2$ μM and $h = 1$ (fixed) (total number of experiments, $n = 31$). On the other hand, nifedipine (10 μM), a blocker of voltage-gated Ca^{2+} channels, showed no effect on the tonic component of the CCh-induced $[Ca^{2+}]_i$ elevation (Figure 7e; similar results were obtained in seven cells). The peak component was also unaffected when the same concentration of nifedipine was added before application of CCh (observed in five cells; data not shown). Essentially the same negative results were obtained if verapamil was used instead of nifedipine (observed in five cells; data not shown).

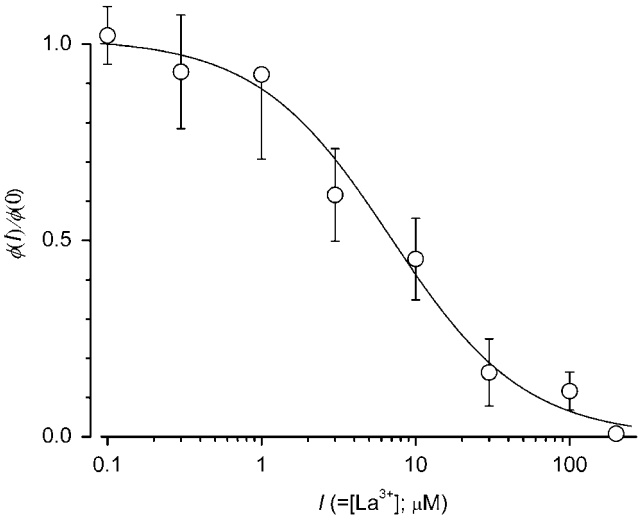

Figure 8 Dose dependence of the inhibitory effect of La^{3+} on the carbachol (CCh)-induced $[Ca^{2+}]_i$ elevation. In the same type of experiments as the one shown in Figure 7d, the inhibitory effect of different concentrations of La^{3+} on the CCh-induced $[Ca^{2+}]_i$ elevation was examined. The continuous line is the best fit of Equation (2) by nonlinear least-squares regression which gave $K = 7$ μM (h was fixed at 1). The ordinate is normalized in terms of $\phi(0)$ determined by the regression. Each symbol represents at least three data. Vertical bars indicate s.e.mean.

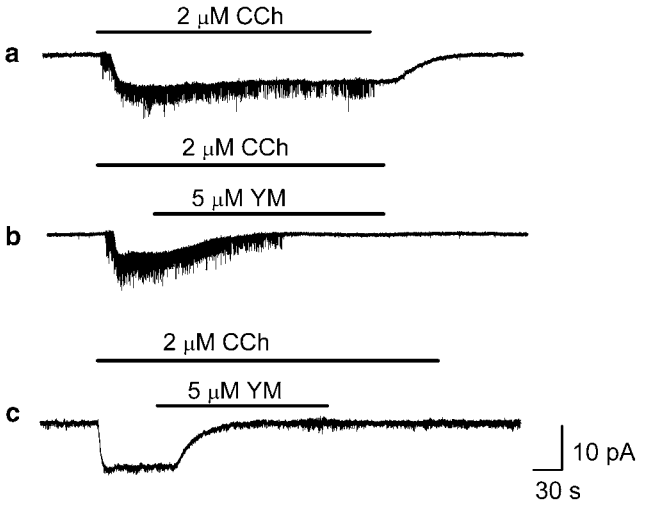

Figure 9 Inhibition of carbachol (CCh)-evoked non-selective cation channel (NSCC) currents by YM-254890 (YM). Whole-cell membrane currents were recorded under voltage clamp at –50 mV using pipettes filled with solution containing 180 μM GTP. (**a**) A typical response of the bovine ciliary muscle cells to CCh. In the majority of the cells, superfusion of 2 μM CCh caused openings of two types of NSCCs (NSCCS and NSCCL) with widely different unitary conductances (100 fS and 35 pS). (**b**) YM inhibited both NSCCL and NSCCS components of a CCh-evoked current. (**c**) A recording from a relatively rare cell in which CCh produced a current almost purely attributable to openings of NSCCS alone. Superfusion of YM (10 μM) abolished the NSCCS current. Recordings (**a**–**c**) are recordings from different cells at 30 °C.

Inhibitory effects of YM on CCh-evoked NSCC currents

Figure 9 illustrates that YM also inhibited NSCC currents evoked by CCh. Whole-cell membrane currents were recorded at 30 °C under voltage clamp at –50 mV using pipettes filled with solution containing 180 μM GTP. In the majority of the cells examined, superfusion of 2 μM CCh caused an inward current accompanied by a clear increase in noise (Figure 9a). We have previously shown that this type of CCh-evoked currents is produced by simultaneous openings of two kinds of NSCC with unitary conductances of 35 pS and 100 fS, which we called NSCCL and NSCCS (see Figure 2 of Takai *et al*., 2004). The large current noise is caused by openings of NSCCL, whereas the downward deflection of the mean current level is mainly attributable to openings of NSCCS (see Takai *et al*., 2004). In some (but not all) cells, CCh-induced openings of NSCCL were clearly observed before the change of the mean current became evident (Figure 9a), supporting the notion that CCh activates two distinct channels. As shown in Figure 9b, both NSCCL and NSCCS components of the CCh-evoked current were completely inhibited by 5 μM YM. Figure 9c shows a recording from a relatively rare cell in which 2 μM CCh produced a current almost purely attributable to openings of NSCCS alone. Superfusion of YM (10 μM) abolished this NSCCS current. Similar results were obtained in six cells that gave an inward current purely attributable to NSCCS openings in response to superfusion of 2 μM CCh. In all cases, there was a time lag of 20–40 s before the inhibitory effect of YM started to appear. The meaning of this time lag is not clear from the present experiments. As was the case with the inhibition of the $[Ca^{2+}]_i$ elevation, relatively high concentrations (>0.5 μM) of YM were required to produce a clear inhibition of the CCh-evoked NSCC currents within 5 min.

Figure 10 shows an example from another set of whole-cell voltage clamp experiments where GTPγS was used to activate the NSCC current. The experimental setup was the same as above, except that the pipettes were filled with solution containing 180 μM GTPγS instead of GTP and had a lower tip resistance (5–8 MΩ). As shown in Figure 10a, spontaneous openings of NSCCL started to be observed 1–2 min after establishment of the whole-cell recording configuration ($t = 0$ min). A clear downward deflection of the mean current level indicating openings of NSCCS was also observed (Figure 10a). In Figure 10b, the $\mu-\sigma^2$ plot resolved two components attributable to NSCCL and NSCCS openings. Similar results were also obtained in 23 other cells. In most of the cells, the NSCCL component of the response lasted for longer than 30 min (Figure 10a). The NSCCS component in contrast quickly decayed and almost disappeared within 10 min in all cells (Figure 10a). In our previous whole-cell clamp experiments, we have also repeatedly noticed that, unlike the NSCCL component, the NSCCS component of CCh-evoked NSCC currents tends to become smaller when stimulation by CCh is repeated (Takai *et al*., 1997, 2004; Sugawara *et al*., 2006). YM (10 μM) had no effect on the NSCC current evoked by GTPγS (Figure 10a; examined in five cells). As the target for the binding of YM is thought to be the step of GDP exchange for GTP in the $G\alpha_{q/11}$ activation states (Takasaki *et al*., 2004), it is expected that non-displaceable binding of GTPγS to $G\alpha_{q/11}$ limits the accessibility of $G\alpha_{q/11}$ to YM.

When we used pipettes with higher tip resistance (12–15 MΩ) to apply GTPγS, the openings of NSCCL started to appear after a longer time lag (5–10 min), and no clear activation of NSCCS was observed (examined in seven cells).

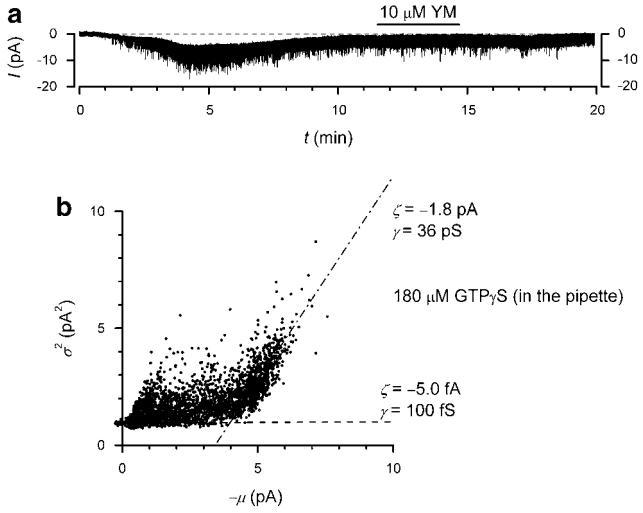

Figure 10 Spontaneous openings of non-selective cation channels (NSCCL and NSCCS) induced by intracellular application of GTPγS, and its insensitivity to YM-254890 (YM). (**a**) Whole-cell current was recorded using pipette filled with solution containing 180 μM GTPγS in place of GTP. The membrane potential was clamped at –50 mV. After establishment of the whole-cell recording configuration ($t = 0$ min), spontaneous openings of NSCCL started to be observed. The clear downward deflection of the mean current level is indicative of simultaneous openings of NSCCS. Note the failure of 10 μM YM to inhibit the GTPγS-induced current. (**b**) Non-stationary variance analysis for the GTPγS-induced current shown in (**a**). The mean current (μ, in pA) and variance (σ^2, in pA^2) were calculated for every 1000 data points of the initial part ($t = 0$ 10 min) of the recording. Lines of the slopes –1.75 pA (dot-dash line) and −4.8 fA (dashed line) are fitted by eye with the two apparently linear components, which probably correspond to openings of NSCCL and NSCCS, respectively.

Immunofluorescence microscopy

Figure 11 shows the results of the immunofluorescence microscopy using the antibody raised against $G\alpha_{q/11}$. In the western blot analysis of total homogenate of bovine ciliary muscle tissue, the anti-$G\alpha_{q/11}$-IgG revealed a clear single band at 42 kDa corresponding to the theoretical molecular mass of $G\alpha_{q/11}$ (Figure 11a, right). Immunostaining with this antibody gave many microscopically visible spots of fluorescence (Figure 11a, left; pseudo-coloured in red; roughly 5–10 spots per square micrometre in the regions of the cell-free plasma membrane preparation, which were also positively stained with the antibody against smooth muscle α-actin (pseudo-coloured in green). As shown in Figure 11b, immunostaining with anti-M_3 receptor-IgG also gave densely distributed punctuated staining (green) in membrane regions where many spots were detected by staining with the anti-$G\alpha_{q/11}$-IgG (red). Omission of the fixation procedure with paraformaldehyde (see Methods) resulted in a marked reduction of binding of the anti-$G_{q/11}$ antibody, whereas it had little effect on the binding of the anti-M_3 receptor antibody (Figure 11c). This is not surprising, because, whereas the M_3 receptor is a true membrane protein with seven transmembrane domains, $G_{q/11}$ is thought to have only relatively loose anchoring to the cytoplasmic side of the plasma membrane (see for example, Watson and Artkinstall, 1994).

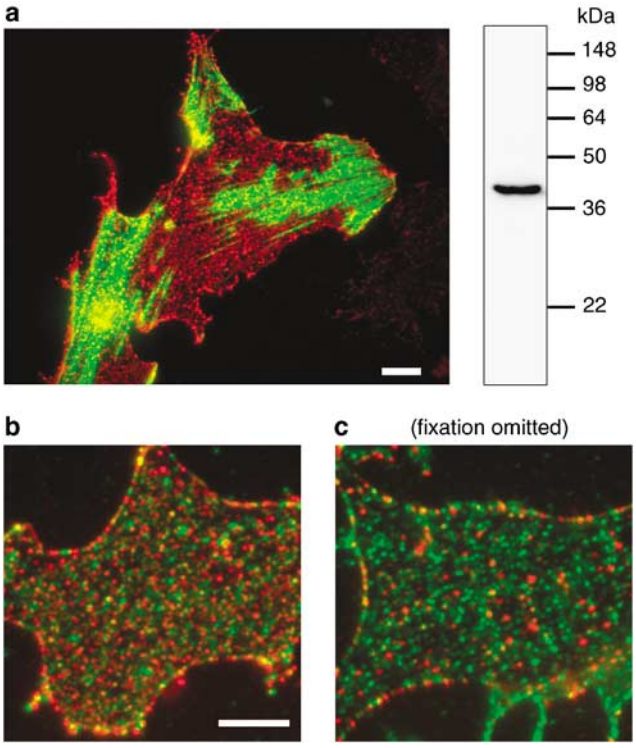

Figure 11 Immunofluorescence microscopy of $G\alpha_{q/11}$ proteins in the plasma membrane of BCM cells. Cell-free plasma membrane preparations on fibronectin-coated glass surface were immunostained for $G\alpha_{q/11}$ (**a**–**c**; pseudo-coloured in red) and, simultaneously, for either α-actin (**a**; green) or M_3 receptor (**b**, **c**; green), using primary antibodies specific to these proteins and AlexaFluor-conjugated secondary antibodies (see Methods). In preparations fixed by pretreatment with 4% paraformaldehyde, the anti-$G\alpha_{q/11}$ antibody gave many microscopically visible (red) spots in the membrane regions that were also stained (in green) with the anti-α-actin antibody (**a**) or anti-M_3 receptor antibody (**b**). Omission of the fixation procedure resulted in a marked reduction of binding of the anti-$G_{q/11}$ antibody, whereas it had little effect on the binding of the anti-M_3 receptor antibody (**c**). Scale bars, 5 μm.

No effects of OAG on the ciliary muscle contractility

Figure 12 illustrates a representative result of the additional mechanical experiments in which we examined the effect of OAG. This membrane-permeable analogue of diacylglycerol (DAG) is known to activate some Ca^{2+}-permeable NSCCs in vascular smooth muscles (reviewed by Albert and Large, 2006). In the ciliary muscle, however, OAG produced no discernible effects on the resting tonus and the contraction evoked by 2 μM-CCh (Figure 12; examined in five muscle bundles). The time course of the relaxation after removal of CCh was not affected, either (Figure 12).

Discussion and conclusion

In the present experiments, we have shown that the $G\alpha_{q/11}$ inhibitor YM inhibits both the initial phasic peak and the ensuing tonic plateau of the contraction (Figures 1, 3 and 4) and associated $[Ca^{2+}]_i$ elevation (Figures 5 and 6) induced by CCh in the bovine ciliary muscle. The inhibition of the phasic component by YM is not unexpected, because there are several lines of evidence that the initial phase of the

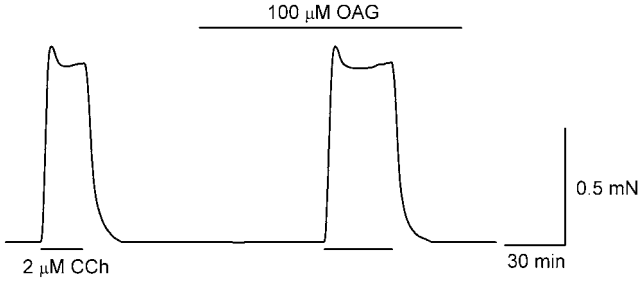

Figure 12 1-Oleyl-2-acetyl-*sn*-glycerol (OAG) exhibits no effects on the contractility. The same method as in Figure 1 was used to record the isometric tension from ciliary muscle bundles. OAG exhibited no discernible effects on the resting tonus and the contraction evoked by superfusion of 2 μM carbachol (CCh).

responses of the ciliary muscle to parasympathetic stimulations is produced by signals sent from M_3 receptors through $G_{q/11}$ to phospholipase Cβ, leading to an increased production of inositol trisphosphate (IP_3) which triggers release of Ca^{2+} from intracellular stores (Stahl *et al*., 1991, 1992; Gupta *et al*., 1994; Takai *et al*., 1997, 2004; Masuda *et al*., 1998; Sugawara *et al*., 2006).

As for the tonic phase of CCh-induced responses, we have previously shown by electrophysiological and mechanical experiments (Takai *et al*., 1997, 2004; Sugawara *et al*., 2006) that Ca^{2+} required for the maintenance of sustained contraction is mainly supplied by influx through two types of M_3 receptor-operated NSCC (NSCCL and NSCCS) in the bovine ciliary muscle, which is known to lack voltage-gated Ca^{2+} channels (Suzuki, 1983). This view is further supported by the present $[Ca^{2+}]_i$ measurements (Figure 7), which have shown that the plateau phase of the $[Ca^{2+}]_i$ elevation evoked by CCh is insensitive to Ca^{2+} channel blockers, whereas it is inhibited by La^{3+} at concentrations ($K = 7$ μM) similar to those ($K = 12$ μM) used to inhibit the CCh-induced NSCC currents (Takai *et al*., 2004).

In the previous whole-cell clamp experiments where we used pipettes with relatively high tip resistance (12–15 MΩ), intracellular application of GTPγS through recording pipette induced a spontaneous opening of NSCCL, but it failed to open NSCCS even at high concentrations (Takai *et al*., 2004). The latter observation then made us consider the possibility that signals from M_3 receptors might reach NSCCS through some novel pathway that is independent of G proteins (Takai *et al*., 2004). However, we have now demonstrated (Figure 9) that the $G\alpha_{q/11}$ inhibitor YM completely suppresses CCh-induced openings of either NSCCL or NSCCS, which have been shown to be insensitive to *Pertussis* toxin, a specific inactivator of $G_{i/o}$ proteins, as well as to cholera toxin, a specific activator of G proteins of the G_s class (Takai *et al*., 2004). We have also shown (Figure 10) that GTPγS causes a transient but clear spontaneous opening of NSCCS, if it is applied through a pipette with a lower tip resistance (5–8 MΩ). The previous failure to detect the activation of NSCCS by GTPγS is thus probably due to masking by a fast concomitant decay. Further, we have confirmed in Figure 11 that $G\alpha_{q/11}$ and M_3 receptors are abundantly distributed in the plasma membrane of the bovine ciliary myocytes or in the vicinity of its cytoplasmic surface. Taken together, the previous and present observations strongly support the notion that, like its phasic component, the tonic component of the contraction of bovine ciliary muscle is under control of signals conveyed from M_3 receptors through a $G_{q/11}$-linked mechanism that communicates in some manner with NSCCs.

Can we propose a similar signalling mechanism involving M_3 receptors, $G_{q/11}$ and NSCCs for the ciliary muscle in mammalian species other than the bovine? The abundant localization of M_3 receptors (or at least of its mRNA) in the ciliary muscle has been reported in the human eye (Pang *et al*., 1993, 1994; Gupta *et al*., 1994; Matsumoto *et al*., 1994) and the monkey eye (Barany *et al*., 1982; Barany, 1985; Gabelt *et al*., 1990; Poyer and Kaufman, 1993) as well as in the bovine eye (Figure 11; see also Masuda *et al*., 1998). The lack or extreme paucity of voltage-gated Ca^{2+} entry pathways has also been demonstrated in the ciliary muscle of the human (Suzuki, 1983) and dog (Ito and Yoshitomi, 1986). It would be interesting to examine the effects of YM on the ciliary muscle of the other mammalian species.

We have previously demonstrated the presence of at least four members of the canonical transient receptor potential protein family (TRPC1, TRPC3, TRPC4 and TRPC6) in the plasma membrane of bovine ciliary muscle cells (Takai *et al*., 2004; Sugawara *et al*., 2006). It is a promising possibility that NACCL and NSCCS are molecular correlates of heteromeric oligomers of these TRPC homologues (Takai *et al*., 2004). Moreover, numerous observations suggest that the TRPCs (particularly TRPC3 and TRPC6) are activated by DAG, one of the two products of the hydrolytic reaction catalysed by phospholipase Cβ (for recent reviews, see Albert and Large, 2006; Hardie, 2007). Although it is tempting to suggest a DAG-mediated mechanism for the NSCC activation in response to M_3 receptor stimulation, we have observed in the present experiments (Figure 11b) that a membrane-permeable DAG analogue, OAG (1–100 μM), exhibits no discernible effects on the resting tension and CCh-induced contraction of bovine ciliary muscle bundles, even after prolonged (>60 min) application. The present experiments have demonstrated that YM is a very useful tool to assess whether $G_{q/11}$ is involved in a signal transduction system, particularly when conventional tools such as GTPγS can provide only limited information. However, it is not possible from the data so far obtained to deduce how the signals are relayed from $G_{q/11}$ to the NSCCs in the bovine ciliary muscle, and further work is needed to address this question.

The release of Ca^{2+} from intracellular stores and its influx from the extracellular space are probably not the only factors that are modulated by the M_3 receptor-$G_{q/11}$ signalling system to control the contraction of the ciliary muscle. As we have shown in the present experiments, contraction induced by 10 μM ionomycin is substantially smaller than that induced by CCh (Figure 2), whereas the $[Ca^{2+}]_i$ is brought up to the saturating level by the same concentration of ionomycin (Figure 5a). Addition of CCh during the plateau phase of the ionomycin-induced contraction causes an increase in the tension, which approaches the tonic level of the contraction produced by CCh alone (Figure 2). The ionomycin-induced contraction augmented by CCh is brought down to, but not below, the level before the addition of CCh by YM (Figure 2). These observations

strongly suggest that signals transmitted by the M_3 receptor-$G_{q/11}$ pathway induce enhancement of the contractility at a given level of $[Ca^{2+}]_i$ (called 'Ca^{2+} sensitization') in the bovine ciliary muscle. Phenomena indicating Ca^{2+} sensitization mediated by trimeric G proteins (mainly of $G_{q/11}$ and $G_{12/13}$ subtypes) activating RhoA/Rho kinase have been reported in various smooth muscles (for reviews, see Sah *et al*., 2000; Somlyo and Somlyo, 2003). The CCh-induced Ca^{2+} sensitization observed in the ciliary muscle may also be, at least partly, mediated by RhoA/Rho kinase. Bacterial toxins and exoenzymes that affect the Rho subfamily of small GTPases (reviewed by Boquet, 1999) have been valuable to investigators of Rho-related systems. Selective inhibitors against Rho kinase, in particular, Y-27632 (Uehata *et al*., 1997), have been shown to be useful in assessing consequences of Rho kinase inhibition (see Sah *et al*., 2000). Experiments using such substances in combination with YM would also be useful to elucidate the Ca^{2+} sensitization mechanism in the ciliary muscle.

Isometric contraction induced by CCh in ciliary muscle bundles is normally maintained for several hours with only a slight decline (Figure 1a). The present examination of the inhibitory effect of YM on this stable contraction has allowed us to demonstrate novel characteristics of the action of YM. We have shown (Figures 1 and 3) that development of the inhibitory effect of YM on the contraction follows a relatively slow time course, and that this tendency of time dependence is particularly marked at lower inhibitor concentrations. Because of this time dependence, it is difficult to estimate accurately the equilibrium dissociation constant K_D for the interaction of YM with $G_{q/11}$ from the concentration–inhibition relationship. However, 30 nM YM inhibits CCh-induced contraction by about 50% within 120 min at 37 °C (Figure 3a). It is therefore rational to assume that $K_D < 30$ nM at this temperature. As the second-order rate constants for the binding of ligands of relatively small molecular size with macromolecules comparable in size to $G_{q/11}$ lie mostly in the range 10^6–$10^8\,M^{-1}s^{-1}$ (see Takai *et al*., 1992), the time constant for the binding of (say) 100 nM YM to $G_{q/11}$ would roughly be estimated to be in the range 0.1–10 s. However, the inhibition of CCh-induced contraction by 100 nM YM follows (after some time lag) a single exponential time course with a time constant of as large as 30 min (= 1800 s; Figure 1c). Therefore, the major rate-limiting step for appearance of the effect of YM is likely to be membrane permeation of YM rather than its binding to $G_{q/11}$.

The temperature dependence is another novel feature of the action of YM revealed by the present experiments (Figure 3). Because the rate coefficients for physical permeation of various hydrophilic and lipophilic solutes through the lipid bilayer of the cell membrane are known to exhibit temperature dependence with Q_{10} values much greater than unity (see Galey *et al*., 1973), it seems reasonable to speculate that the lower sensitivity of the ciliary muscle to YM at 25 °C compared with 37 °C (Figure 3) is due in part to a reduction of the membrane permeability to YM. In the present $[Ca^{2+}]_i$ measurements (Figure 5) and electrophysiological experiments (Figure 9), relatively high concentrations of YM were required to obtain clear inhibitory effects. This may at least partly be explained by the fact that these experiments were carried out at room temperature (25 °C).

Acknowledgements

This study was supported by Grants-in-Aid from the Ministry of Education, Culture, Sports, Science and Technology of Japan (nos. 17659059 and 19590202). We thank Dr Richard J Lang (Monash University, Australia) for reading the first version of the paper before submission.

Conflict of interest

The authors state no conflict of interest.

References

Albert AP, Large WA (2006). Signal transduction pathways and gating mechanisms of native TRP-like cation channels in vascular myocytes. *J Physiol* **570**: 45–51.

Alexander SPH, Mathie A, Peters JA (2007). Guide to receptors and channels (GRAC), 2nd edition (2007 revision). *Br J Pharmacol* **150** (Suppl 1): S1–S168.

Barany E, Berrie CP, Birdsall NJ, Burgen AS, Hulme EC (1982). The binding properties of the muscarinic receptors of the cynomolgus monkey ciliary body and the response to the induction of agonist subsensitivity. *Br J Pharmacol* **77**: 731–739.

Barany EH (1985). Muscarinic subsensitivity without receptor change in monkey ciliary muscle. *Br J Pharmacol* **84**: 193–198.

Boquet P (1999). Bacterial toxins inhibiting or activating small GTP-binding proteins. *Ann NY Acad Sci* **886**: 83–90.

Carroll RJ, Ruppert D (1988). *Transformation and Weighting in Regression*. Chapman and Hall: New York, USA.

Gabelt BT, Kaufman PL, Polansky JR (1990). Ciliary muscle muscarinic binding sites, choline acetyltransferase, and acetylcholinesterase in aging rhesus monkeys. *Invest Ophthalmol Vis Sci* **31**: 2431–2436.

Galey WR, Owen JD, Solomon AK (1973). Temperature dependence of nonelectrolyte permeation across red cell membranes. *J Gen Physiol* **61**: 727–746.

Glasser A, Kaufman PL (2003). Accommodation and presbyopia. In: Kaufman PL, Alm A (eds). *Adler's Physiology of the Eye: Clinical Application*. Mosby: St Louis, pp 197–233.

Gupta N, Drance SM, McAllister R, Prasad S, Rootman J, Cynader MS (1994). Localization of M_3 muscarinic receptor subtype and mRNA in the human eye. *Ophthalmic Res* **26**: 207–213.

Hardie RC (2007). TRP channels and lipids: from *Drosophila* to mammalian physiology. *J Physiol* **578**: 9–24.

Ito Y, Yoshitomi T (1986). Membrane and contractile properties of the dog ciliary muscle. *Br J Pharmacol* **88**: 629–638.

Masuda H, Goto M, Tamaoki S, Kamikawatoko S, Tokoro T, Azuma H (1998). M3-type muscarinic receptors predominantly mediate neurogenic quick contraction of bovine ciliary muscle. *Gen Pharmacol* **30**: 579–584.

Matsumoto S, Yorio T, DeSantis L, Pang IH (1994). Muscarinic effects on cellular functions in cultured human ciliary muscle cells. *Invest Ophthalmol Vis Sci* **35**: 3732–3738.

Pang IH, Matsumoto S, Tamm E, DeSantis L (1994). Characterization of muscarinic receptor involvement in human ciliary muscle cell function. *J Ocul Pharmacol* **10**: 125–136.

Pang IH, Shade DL, Tamm E, DeSantis L (1993). Single-cell contraction assay for human ciliary muscle cells. Effect of carbachol. *Invest Ophthalmol Vis Sci* **34**: 1876–1879.

Poyer JF, Kaufman PL (1993). Effect of muscarinic agonists and receptor subtype-specific antagonists on the contractile responses of the isolated rhesus monkey ciliary muscle. *Invest Ophthalmol Vis Sci* **34**: 921S.

Sah VP, Seasholtz TM, Sagi SA, Brown JH (2000). The role of Rho in G protein-coupled receptor signal transduction. *Annu Rev Pharmacol Toxicol* **40**: 459–489.

Sigworth FJ (1980). The variance of sodium current fluctuations at the node of Ranvier. *J Physiol* **307**: 97–129.

Snedecor GW, Cochran WG (1980). *Statistical Methods*, 7th edn. Iowa State University Press: Ames, Iowa, USA.

Somlyo AP, Somlyo AV (2003). Ca^{2+} sensitivity of smooth muscle and nonmuscle myosin II: modulated by G proteins, kinases, and myosin phosphatase. *Physiol Rev* **83**: 1325–1358.

Stahl F, Gebauer B, Lepple-Wienhues A, Langenbeck-Groh G, Berweck S, Wiederholt M (1992). Characterization of acetylcholine- and endothelin-induced calcium entry in cultured human ciliary muscle cells. *Pflügers Arch* **422**: 105–111.

Stahl F, Lepple Wienhues A, Kuppinger M, Schneider U, Wiederholt M (1991). Measurements of intracellular calcium and contractility in human ciliary muscle. *Pflügers Arch* **418**: 531–537.

Sugawara R, Takai Y, Miyazu M, Ohinata H, Yoshida A, Takai A (2006). Agonist and antagonist sensitivity of non-selective cation channel currents evoked by muscarinic receptor stimulation in bovine ciliary muscle cells. *Auton Autacoid Pharmacol* **26**: 285–292.

Suzuki R (1983). Neuronal influence on the mechanical activity of the ciliary muscle. *Br J Pharmacol* **78**: 591–597.

Takahashi A, Camacho P, Lechleiter JD, Herman B (1999). Measurement of intracellular calcium. *Physiol Rev* **79**: 1089–1125.

Takai A, Ohno Y, Yasumoto T, Mieskes G (1992). Estimation of the rate constants associated with the inhibitory effect of okadaic acid on type 2A protein phosphatase by time course analysis. *Biochem J* **287**: 101–106.

Takai Y, Awaya S, Takai A (1997). Activation of non-selective cation conductance by carbachol in freshly isolated bovine ciliary muscle cells. *Pflügers Arch* **433**: 705–712.

Takai Y, Sugawara R, Ohinata H, Takai A (2004). Two types of non-selective cation channel opened by muscarinic stimulation with carbachol in bovine ciliary muscle cells. *J Physiol* **559**: 899–922.

Takasaki J, Saito T, Taniguchi M, Kawasaki T, Moritani Y, Hayashi K *et al*. (2004). A novel $G\alpha_{q/11}$-selective inhibitor. *J Biol Chem* **279**: 47438–47445.

Uehata M, Ishizaki T, Satoh H, Ono T, Kawahara T, Morishita T *et al*. (1997). Calcium sensitization of smooth muscle mediated by a Rho-associated protein kinase in hypertension. *Nature* **389**: 990–994.

Uemura T, Kawasaki T, Taniguchi M, Moritani Y, Hayashi K, Saito T *et al*. (2006). Biological properties of a specific $G\alpha_{q/11}$ inhibitor, YM-254890, on platelet functions and thrombus formation under high-shear stress. *Br J Pharmacol* **148**: 61–69.

Watson S, Artkinstall S (1994). *The G-Protein Linked Receptor*. Academic Press: London, UK.

Williams DA, Fogarty KE, Tsien RY, Fay FS (1985). Calcium gradients in single smooth muscle cells revealed by the digital imaging microscope using Fura-2. *Nature* **318**: 558–561.